Australasian Universities Power Engineering Conference
M. Negnevitsky, ed., Hobart, Australia, September 25 - 28, 2005

# Determination of Winding Inductance in a Claw Pole Permanent Magnet Motor with SMC Core

YouGuang GUO[1], Jian Guo ZHU[1], Haiwei LU[1], Ram CHANDRU[1], Shuhong, WANG[1,2], and Jianxun JIN[3]
[1]Faculty of Engineering, University of Technology, Sydney, NSW 2007, Australia
[2]Institute of Electrical Engineering, Xi'an Jiaotong University, Xi'an, China
[3]School of Automation Engineering, U. of Electronic Sci. & Tech. of China, Chengdu, China
youguang@eng.uts.edu.an, joe@eng.uts.edu.au

## ABSTRACT

*This paper presents the investigation on the winding inductances of a claw pole permanent magnet motor with soft magnetic composite (SMC) stator by numerical magnetic field analysis. The inductance is computed with different stator currents and rotor positions by various approaches, and the results are compared and analysed. The inductance is one of the key parameters determining the motor performance, and the accurate information of the inductances versus geometry and saturation saliencies is very useful for the design of high performance motor and control scheme. The theoretical calculations are verified by experimental results.*

## 1. INTRODUCTION

Soft magnetic composite (SMC) material and its application in electromagnetic devices have achieved significant progress in the past decade due to the material's unique properties, including isotropic magnetic and thermal properties, very low eddy current loss and relatively low total loss at medium and higher frequencies, nearly net-shape fabrication process with fine tolerance and surface smooth, and the prospect of low cost mass production [1]. It is anticipated by some researchers that SMC application could lead to a revolution of electrical machine manufacturing industry [2]. In particular, the isotropic magnetic property creates crucial design benefits and radical topologies can be exploited to obtain high machine performance because the magnetic flux does not have to be constrained in a two-dimensional (2D) plane like electrical steels, commonly used in transformers and rotating electrical machines. Typical examples of SMC application are claw pole and transverse flux machines [3, 4].

For such electrical machines with complex structure and new materials, accurate parameter prediction is crucial in the design stage. This paper presents the determination of winding inductance in a claw pole permanent magnet (PM) motor with SMC stator core by finite element analysis (FEA).

Considering the complex motor topology and magnetic field distribution, three-dimensional (3D) nonlinear FEA of magnetic field is performed using a comprehensive commercial software ANSYS. The winding inductance is calculated with various stator currents and rotor positions by different approaches, and the results are compared and analysed. The calculations are validated by the experimental results.

## 2. CLAW POLE SMC MOTOR

To investigate the application of SMC in electrical machines, a three-phase three-stack claw pole motor with SMC stator core has been designed by fully taking the advantage of the unique properties of the new material, particularly the 3D magnetic isotropy [5, 6]. For example, the magnet is designed to be axially longer than the claw pole as the magnetic flux produced by PMs can flow into the claw poles via the side surfaces. The motor has been successfully operated with a sensorless brushless DC drive scheme, delivering an output of 500 W at 1800 rev/min when a current of 4.1 A *rms* flows into the stator winding.

Figure 1 illustrates the magnetically relevant parts of the motor and Table 1 lists the major dimensions and parameters. The three phases are stacked axially and shifted to each other by 120° electrical. Each stator phase has a single coil around an SMC core, which is moulded in two halves. The outer rotor comprises a tube of mild steel with an array of magnets for each phase mounted on the inner surface. Mild steel is used for the rotor because the flux density in the yoke is almost constant.

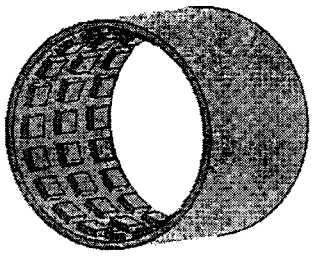

(a) Rotor

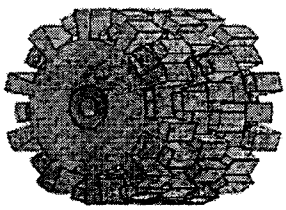

(b) Three-stack stator cores

Figure 1: Magnetically relevant parts of the claw pole SMC motor.

TABLE I
MAJOR DIMENSIONS AND PARAMETERS

| Dimensions and parameters | Quantities |
|---|---|
| Rated frequency (Hz) | 300 |
| Number of phases | 3 |
| Rated power (W) | 500 |
| Rated line-to-neutral voltage (V) | 64 |
| Rated phase current (A) | 4.1 |
| Rated speed (rev/min) | 1800 |
| Rated torque (Nm) | 2.65 |
| Rated efficiency (%) | 81.5 |
| Rated temperature rise (°C) | 75 |
| Number of poles | 20 |
| Stator core material | SOMALOY™ 500 |
| Stator outer radius (mm) | 40 |
| Effective stator axial length (mm) | 93 |
| Total motor length (mm) | 137 |
| Rotor (and motor) outer radius (mm) | 47 |
| Rotor inner radius (mm) | 41 |
| Permanent magnets | NdFeB, Grade N30M |
| Number of magnets | 60 |
| Magnet dimensions | OD88 x ID82 x 15 mm arc 12° |
| Magnetization directions | Radially outward and inward |
| Main airgap length (mm) | 1 |
| Stator shaft material | Mild steel |
| Shaft outer radius (mm) | 9 |
| Number of coils | 3 |
| Coil window dimension ($mm^2$) | 17 x 11 |
| Number of turns | 75 |

## 3. 3D FEA OF MAGNETIC FIELD

To design and analyse electrical machines, equivalent electric circuit is often used to predict the motor performance. The machine is represented by lumped parameters such as rotational electromotive force (*emf*), resistance and inductance, which can be calculated analytically or numerically. The analytical approach (or the equivalent magnetic circuit method) is based on some simplifying assumptions including linear magnetic material, idealised core and winding geometry. However, the calculation is sometimes far from accurate, especially for the machines with complex structure and high saturation. A more accurate method, e.g. the numerical analysis by finite element method (FEM), is therefore required to improve the computational accuracy. Magnetic field analysis by FEM can take into account the actual distribution of windings, geometry details, and the non-linearity of magnetic materials of the electrical machine.

Due to the independence of magnetic flux paths between phases and the symmetry of structure, only a pole-pitch region is required for the magnetic field FEA, as shown in Figure 2.

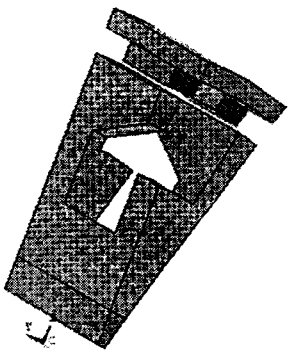

Figure 2: Region for field solution

At the two radial boundary planes, the magnetic scalar potential obeys the so-called half-periodical boundary conditions by

$$\varphi_m(r, \Delta\theta/2, z) = -\varphi_m(r, -\Delta\theta/2, -z) \quad (1)$$

where $\Delta\theta$ = 18° is the angle of one pole pitch. The original point of the cylindrical coordinate is located at the centre of the stack.

Figure 3 illustrates the no-load flux density vectors with line lengths proportional to the magnitudes at rotor position $\theta$ = 0°, defined as where the magnets share the same axes as the stator claw poles respectively. It is shown that the major path of the magnetic flux of the PMs is along one of the PMs – the main air gap – one of the SMC claw pole stator core pieces – the SMC stator yoke – another SMC claw pole stator core piece – main airgap – another PM and then – the mild steel rotor yoke to form a closed loop. There is also a significant amount of flux leakage, particularly between the side surfaces of the claw poles, though it is unwanted. Both the major and leakage paths are three-dimensional. Figure 4 plots the flux density vectors generated by the rated stator current only, showing that the major path of armature reaction is not the same as that of the PM flux.

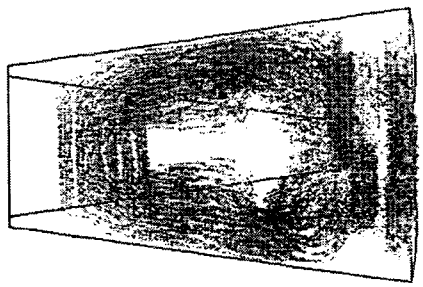

Figure 3: Magnetic flux density vectors at no-load

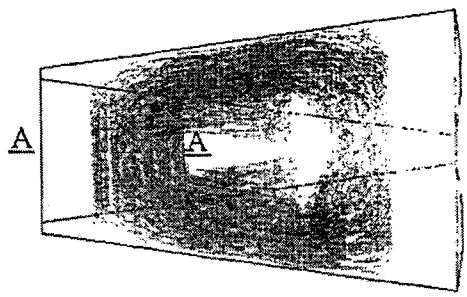


Figure 4: Magnetic flux density vectors generated by stator current only.

## 4. INDUCTANCE CALCULATION AND MEASUREMENT

### 4.1. FEA WITH STATOR CURRENT ONLY

The self-inductance of the stator winding, $L$, can be evaluated by the two conventional approaches, i.e. the flux-linkage method as

$$L = \frac{\lambda}{i} = \frac{N\phi}{i} \quad (2)$$

or the energy method as

$$L = \frac{2W_f}{i^2} \tag{3}$$

where $\lambda$, $\phi$ and $W_f$ are the magnitudes of the flux-linkage and flux linking the winding, and the magnetic co-energy stored in the whole machine, respectively, produced by a current $i$ in each of $N$ turns. The flux and magnetic co-energy can be obtained from the results of a field analysis with a current $i$ while the PMs are "switched off", i.e. remanence is set to zero. The mutual inductance between phases can be considered as zero because of the almost independent magnetic flux paths.

A difficulty with the flux-linkage method is the accurate determination of the flux flowing through the stator winding. Theoretically, the flux can be computed by the surface integral of flux density $B$, or the loop integral of vector potential $A$ after the magnetic field distribution is solved by FEA, but it is not easy to define a proper integration surface or path when the winding is not a simple loop and is of non-negligible size. For this claw pole motor, the winding flux can be approximately calculated based on the middle cross-sectional area of the stator yoke, marked as A-A in Figure 4.

Figure 5 plots the computed inductances versus rotor angle with $i$ = 0.041 A (1% the rated current) and 4.1A, respectively. It can be seen that the inductance is almost constant for different rotor positions since the motor has a quite big equivalent airgap and the major path of the armature reaction is almost the same, as shown in Figure 4. It is also noticed that the inductance reduction due to armature reaction is small since the magnetic circuit does not saturate deeply due to the stator current only.

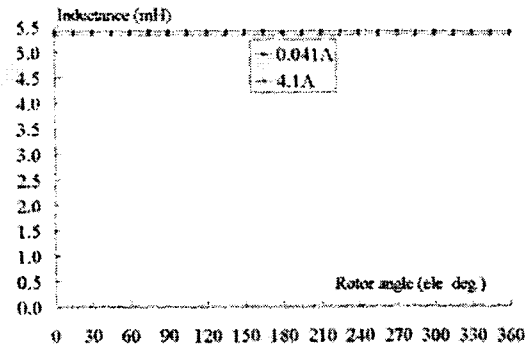


Figure 5: Computed Inductance using the flux-linkage method based on the magnetic field generated by stator current only.

By contrast, the energy method can avoid the difficulty of choosing the proper integration geometry. It calculates the energy or co-energy stored in all the elements and is considered as quite accurate because the principle of FEA is based on the minimization of magnetic field energy. In this paper, the investigation on the winding inductance is mainly carried out by the energy method. Figure 6 shows the computed self-inductance of one phase winding versus rotor angle at no-load and full-load. The results are quite close to those by the flux-linkage method and the difference may be caused by the selection of flux integration area (in the flux-linkage method) and computational error.

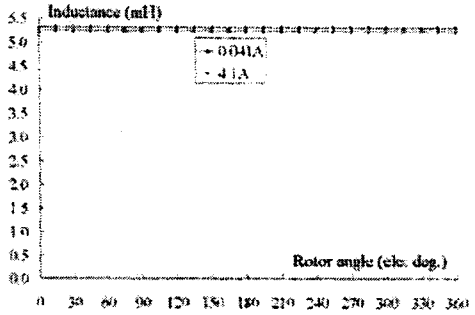


Figure 6: Computed Inductance using the energy method based on the magnetic field generated by stator current only.

However, the analysis with the winding excitation only cannot provide the "true" inductance when the magnetic circuit is saturated. The saturation levels and the "true" flux or energy contributed by the current $i$ are different with the individual excitation or with the "true" condition of multiple excitations.

### 4.2. Saturation Determined by Both Stator Current and PMs

To consider the saturation caused by both the stator current and PMs, two-step analyses are carried out, i.e. a non-linear analysis with the excitations of both PMs and armature current $i$ for saving the permeability of each element, and then a linear analysis with a stator current only and the saved permeabilities is performed to find the $\phi$ in (2) or the $W_f$ in (3).

Under the condition of the optimum brushless DC control, the stator current is in phase with the back *emf*, i.e. lagging the PM flux (defined as the winding flux produced by PMs) by 90 degrees electrical. The fundamental of the stator current can be determined by

$$i = \sqrt{2} I_{rms} \sin\theta \tag{4}$$

where $I_{rms}$ is the *rms* value of the stator current (4.1A for full-load), $\theta$ is the rotor angle with the zero position where the claw poles line up with the rotor PMs, as shown in Figure 2.

The calculated phase winding inductance ($L_{sec}$) versus different rotor angle and load is shown in Figure 7.

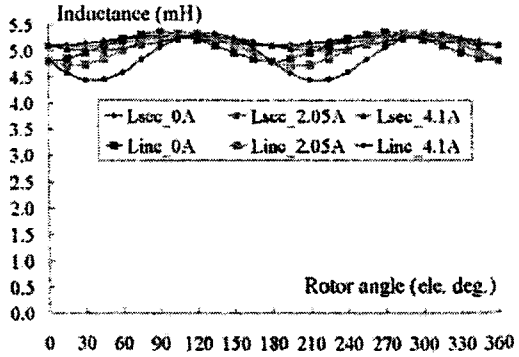


Figure 7: Computed secant and incremental inductances while FEA considers the saturation caused by both stator current and PMs.

This calculation is in fact the secant (or apparent) inductance, i.e. the slope of the linearised characteristic of flux-linkage versus current through the origin and the operating point, as shown in Figure 8.

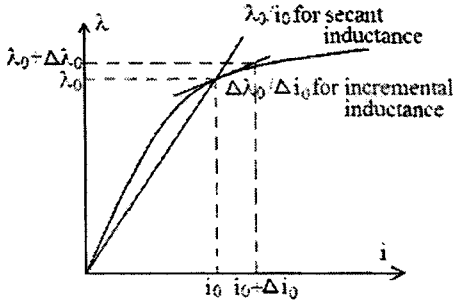


Figure 8: Flux-linkage versus current

### 4.3. INCREMENTAL INDUCTANCE

The behaviour of an electric circuit is governed by the so-called incremental (or differential) inductance, along the tangential line at the operating point, as illustrated in Figure 8. The governing equation of one phase winding can be written as

$$u = Ri + \frac{d\lambda}{dt} \tag{5}$$

where $u$, $R$, $i$ and $\lambda$ are the voltage, resistance, current and flux linkage of the winding, respectively. The flux linkage, contributed by both the stator current and PMs, varies with stator current $i$ and rotor position $\theta$ as

$$\lambda = \lambda(i, i_{m1}, i_{m2}, \cdots i_{mp}, \theta) \tag{6}$$

where $i_{m1}$, $i_{m2}$, ..., $i_{mp}$ are the currents of the equivalent coils of magnets, respectively, and $p$ is the number of magnets of one stack. Substituting (6) into (5) and applying the chain rule of the flux linkage, the voltage can be expressed as

$$\begin{aligned} u &= Ri + \frac{\partial\lambda}{\partial i}\frac{di}{dt} + \frac{\partial\lambda}{\partial\theta}\frac{d\theta}{dt} \\ &= Ri + L_{inc}\frac{di}{dt} + E \end{aligned} \tag{7}$$

where $L_{inc}=\partial\lambda/\partial i$ is the incremental inductance, and $E$ is the rotational *emf*. Note that the currents of the equivalent coils of magnets are constants, so their derivatives are zero.

#### 4.3.1. INCREMENTAL ENERGY METHOD

The calculation of $L_{inc}$ involves calculating the increment of flux-linkage due to a small perturbation of current. To avoid the difficulty in defining the integration geometry for flux-linkage computation, the incremental energy method (IEM) is often used [7, 8]. IEM computes the inductance using the magnetic field FEA in conjunction with energy/current perturbation.

For a lossless (conservative) magnetic system, the sum of magnetic energy $W$ and co-energy $W_c$ is given by

$$W + W_c = \lambda i + \lambda_{m1} i_{m1} + \lambda_{m2} i_{m2} + \cdots + \lambda_{mp} i_{mp} \tag{8}$$

By differentiating the both sides of the above equation, the follows can be obtained

$$\begin{aligned} dW + dW_c = {} & id\lambda + \lambda di \\ & + i_{m1} d\lambda_{m1} + i_{m2} d\lambda_{m2} + \cdots + i_{mp} d\lambda_{mp} \\ & + \lambda_{m1} di_{m1} + \lambda_{m2} di_{m2} + \cdots + \lambda_{mp} di_{mp} \end{aligned} \tag{9}$$

or

$$dW = id\lambda + i_{m1} d\lambda_{m1} + i_{m2} d\lambda_{m2} + \cdots + i_{mp} d\lambda_{mp} \tag{10a}$$

$$dW_c = \lambda di + \lambda_{m1} di_{m1} + \lambda_{m2} di_{m2} + \cdots + \lambda_{mp} di_{mp} \tag{10b}$$

The differential can also be expressed as

$$dW_c = \frac{\partial W_c}{\partial i} di + \frac{\partial W_c}{\partial i_{m1}} di_{m1} + \frac{\partial W_c}{\partial i_{m2}} di_{m2} + \cdots + \frac{\partial W_c}{\partial i_{mp}} di_{mp} \tag{11}$$

Comparing (10b) and (11) revels that

$$\lambda = \frac{\partial W_c}{\partial i} \tag{12}$$

Then, the incremental self-inductance formulation using the energy/current perturbation method can be written as

$$\begin{aligned} L_{inc} &= \frac{\partial\lambda}{\partial i} = \frac{\partial^2 W_c}{\partial i^2} \\ &\approx \frac{W_c(i+\Delta i) + W_c(i-\Delta i) - 2W_c(i)}{(\Delta i)^2} \end{aligned} \tag{13}$$

This is the general IEM formula, proposed in [7, 8]. It seems that two incremental analyses are required for self-inductance (and four for mutual ones) [9]. In fact, (13) can be reduced to a very simple form, requiring one incremental analysis only.

For linear analysis, the stator current $i$ can be any value, i.e. 0. With a current perturbation $\Delta i$ only (from zero current), this formula can be reduced to

$$L_{inc} \approx \frac{2\Delta W_c}{(\Delta i)^2} \tag{14}$$

where $\Delta W_c$ is the increment of magnetic co-energy, which equals the energy in the linear analysis.

In summary, the modified IEM (MIEM) calculates the incremental inductance by the following steps: (I) Perform non-linear magnetic field analysis with the excitation of both the stator current and PMs; (II) Determine and save the differential permeability in each element; (III) Conduct linear analysis with the saved differential permeabilities and a perturbed current only; (IV) Calculate the co-energy increment and then the incremental inductance by (14). In fact, the perturbed current in (III) can be large since the magnetic field analysis is linear.

#### 4.3.2. ENHANCED INCREMENTAL ENERGY METHOD

To improve the accuracy and computational efficiency of the IEM (13), which requires two incremental analyses for self-inductance (and four for mutual ones),

Gyimesi and Ostergaard introduced the so-called enhanced incremental energy method (EIEM) [9].

The stored magnetic energy supplied by the electric circuit of the phase winding can be obtained by

$$W = \int (u - Ri - E) i dt = \int L_{inc} i di = \int L_{inc} \frac{d(i^2)}{2} \qquad (15)$$

The incremental self-inductance is then calculated by

$$L_{inc} = 2\frac{dW}{d(i^2)} \qquad (16)$$

Like the calculation of secant inductance, the first step is a non-linear analysis to obtain the operating point solution. However, the next step is to determine the differential permeabilities, rather than the apparent ones. Then, a linear analysis is performed with the saved differential permeabilities. When the current is perturbed by an increment $\Delta i_0$ from the operating point $i_0$ (can be any value for linear analysis, e.g. the simplest is 0), the energy increment can be evaluated as

$$\Delta W = L_{inc} \frac{(i_0 + \Delta i_0)^2 - i_0^2}{2} = L_{inc} \frac{(\Delta i_0)^2 + 2 i_0 \Delta i_0}{2} \qquad (17)$$

Assume $\mathbf{B}_0$ and $\mathbf{H}_0$ are the operating flux density and field strength in an element when the motor is excited by a stator current $i_0$ and PMs ($i_{m1}$, $i_{m2}$, ...$i_{mp}$), the field variation $\Delta\mathbf{B}_0$ and $\Delta\mathbf{H}_0$ due to the current perturbation, $\Delta i_0$, has the following relationship

$$\Delta \mathbf{B}_0 = \mu_d \Delta \mathbf{H}_0 \qquad (18)$$

where $\mu_d$ is the differential permeability at the operating point of the B-H curve. The energy increment is

$$\begin{aligned} \Delta W &= \sum_{e=1}^{N_e} \frac{(B_0 + \Delta B_0)(H_0 + \Delta H_0) - B_0 H_0}{2} V_e \\ &= \sum_{e=1}^{N_e} \frac{\Delta B_0 \Delta H_0 + 2 H_0 \Delta B_0}{2} V_e \end{aligned} \qquad (19)$$

where $N_e$ is the number of elements and $V_e$ is the volume of the e-th element. By comparing (17) and (19), the incremental inductance can be calculated by

$$L_{inc} = \frac{\sum_{e=1}^{N_e} \Delta B_0 \Delta H_0 V_e}{(\Delta i_0)^2} \qquad (20)$$

It is noted that the difference between EIEM (20) and IEM (13) is with the calculation of incremental energy and inductance formula. The major improvement by EIEM includes: (I) Only one incremental analysis is required; (II) The current perturbation can be large as the incremental analysis is linear; (III) The energy calculation does not incorporate the B-H curve, avoiding the evaluation of absolute non-linear energy in EIEM.

In fact, the so-called EIEM is the same as the formula (14), the MIEM, which is applied in this paper to compute the incremental inductance of the phase winding at different rotor positions and loads, as shown in Figure 7. Comparing to the secant counterpart, the incremental inductance generally has smaller values and varies more drastically. This agrees with the slopes of the cord and tangential lines in Figure 8.

### 4.4. Inductance Measurement

For measurement of the inductance, a small AC current (0.2 A, 500 Hz) was fed into the phase winding when the rotor is locked. The voltage across the two terminals, $V_1$, and the current flowing through the winding, $I_1$, are measured. The phase winding inductance can be calculated by

$$L_1 = \sqrt{(V_1 / I_1)^2 - R_1^2} / (2\pi f_1) \qquad (21)$$

where $f_1$ is the frequency, and $R_1$ is the resistance of the phase winding. The inductances are measured at different rotor positions, as shown in Figure 9. For comparison, the computed secant and incremental inductances at no-load are also shown in the figure. The computations agree with the measurements. Some error may be caused by the measuring current, which causes a small loop in the vicinity of the saturation point in the B-H curve. Another possible reason is the eddy current caused by the measuring current. Although the particles of SMC materials have been coated by a thin electrical insulation, the eddy current might be non-negligible due to the possible insulation damage during the high pressure compaction process. Ideally, the measuring current should be as close to zero as possible but the reading error could be large.

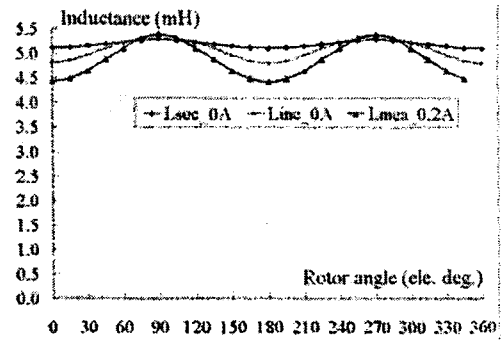


Figure 9: Computed and measured inductances

### 4.5. Inductances with a DC Current Bias

When the electrical machine operates in synchronous steady state, its magnetomotive force (*mmf*) produced by the armature current, or the resulting *mmf* by both the armature current and PMs, leads or lags the PM *mmf* by a fixed angle. Referred to the rotor, the stator current can be seen as a DC at a specified load. Therefore, the inductance pattern versus different stator currents and rotor positions are very useful information for the design of high performance control scheme, e.g. the direct torque control. Figure 10 plots the computed incremental inductance of the phase winding against rotor position (0 to 360 electrical degrees at the interval of 15) and stator current (0 to 4 A with 1 A interval). These data, in combination with the interpolation technique, could provide a useful look-up table for the control scheme of the motor.

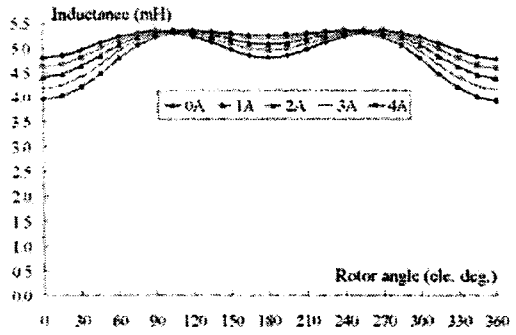


Figure 10: Computed incremental inductances with DC bias in the stator winding

Figure 11 shows the measured inductances against rotor position with DC bias of 0A, 2A and 4A, respectively. The calculated counterparts are replotted in the figure for comparison, showing that the calculations agree with the measurements.

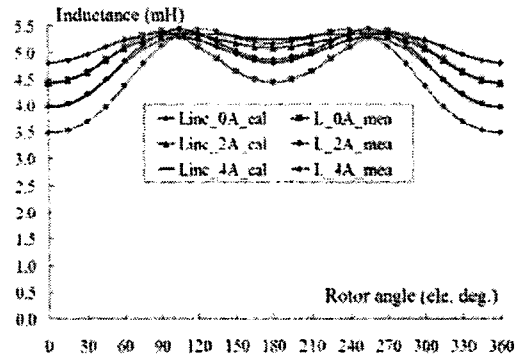


Figure 11: Measured and calculated inductances with DC bias (0A, 2A, or 4A) in the stator winding

## 5. CONCLUSIONS

This paper investigated the winding inductance of a permanent magnet claw pole motor with SMC stator core by finite element magnetic field analysis. Various methods for the calculation of winding inductances (secant and incremental) are reviewed and analysed. Based on the IEM, a modified method (MIEM) was proposed and applied to compute the winding inductance of the claw pole SMC motor versus different rotor positions and stator currents, which could provide useful information for the design of high performance control scheme. The inductance computations have been validated by the measurements on the prototype.

## REFERENCES

[1] "The Latest Development in Soft Magnetic Composite Technology," *SMC Update, Reports of Höganäs AB, Sweden,* 1997-2005. Available at http://www.hoganas.com/, see News then SMC Update.

[2] A.G. Jack, "Experience with the Use of Soft Magnetic Composites in Electrical Machines," in Proc. Int. Conf. on Electrical Machines, Istanbul, Turkey, pp1441-1448, Sept. 1998.

[3] Y.G. Guo, J.G. Zhu, P.A. Watterson, and W. Wu, "Comparative Study of 3-D Flux Electrical Machines with Soft Magnetic Composite Core," IEEE Trans. Ind. Applicat., vol.39, pp1696-1703, 2003.

[4] J.G. Zhu and Y.G. Guo, "Study with Magnetic Property Measurement of Soft Magnetic Composite Material and Its Application in Electrical Machines," in Proc. 39th IEEE Industry Application Society Annual Meeting, Seattle, USA, pp373-380, Oct. 2004.

[5] Y.G. Guo, J.G. Zhu, P.A. Watterson, W.M. Holliday, and W. Wu, "Improved Design and Performance Analysis of a Claw Pole Permanent Magnet SMC Motor with Sensorless Brushless DC Drive," in Proc. 5th IEEE Int. Conf. Power Electronics and Drive Systems, Singapore, pp704-709, Nov. 2003.

[6] Y.G. Guo, J.G. Zhu, P.A. Watterson, and W. Wu, "Development of a Claw Pole Permanent Magnet Motor with Soft Magnetic Composite Stator," Australian J. of Electrical & Electronic Eng., vol.2, pp21-30, 2005.

[7] N.A. Demerdash and T.W. Nehl, "Electrical Machinery Parameters and Torques by Current and Energy Perturbations from Field Computations – Part I: Theory and Formulation," IEEE Trans. Energy Conversion, vol.14, pp1507-1513, 1999.

[8] N.A. Demerdash and T.W. Nehl, "Electrical Machinery Parameters and Torques by Current and Energy Perturbations from Field Computations – Part II: Applications and Results," IEEE Trans. Energy Conversion, vol.14, pp1514-1522, 1999.

[9] M. Gyimesi and D. Ostergaard, "Inductance Computation by Incremental Finite Element Analysis," IEEE Trans. Magn., vol.35, pp1119-1122, 1999.